THE ASTROPHYSICAL JOURNAL, 443:64–76, 1995 April 10

THE EVOLUTION OF C/O IN DWARF GALAXIES FROM *HUBBLE SPACE TELESCOPE* FOS OBSERVATIONS[1]

DONALD R. GARNETT[2] AND EVAN D. SKILLMAN
Astronomy Department, University of Minnesota, 116 Church Street, S.E., Minneapolis, MN 55455;
garnett@oldstyle.spa.umn.edu, skillman@zon.spa.umn.edu

REGINALD J. DUFOUR
Department of Space Physics and Astronomy, Rice University, Houston, TX 77251-1892

MANUEL PEIMBERT AND SILVIA TORRES-PEIMBERT
Instituto de Astronomia, UNAM, Apartado Postal 70-264, DF 04510 Mexico, Mexico

ROBERTO TERLEVICH AND ELENA TERLEVICH
Royal Greenwich Observatory, Madingley Road, Cambridge CB30EZ, England, UK

AND

GREGORY A. SHIELDS
Astronomy Department, University of Texas, Austin, TX 78712
Received 1994 June 28; accepted 1994 October 18

ABSTRACT

We present UV observations of seven H II regions in low-luminosity dwarf irregular galaxies and the Magellanic Clouds obtained with the Faint Object Spectrograph on the *Hubble Space Telescope* (*HST*) in order to measure the C/O abundance ratio in the interstellar medium (ISM) of those galaxies. We measure both O III] 1666 Å and C III] 1909 Å in our spectra, enabling us to determine C^{+2}/O^{+2} with relatively small uncertainties. The results from our *HST* observations show a continuous increase in C/O with increasing O/H, consistent with a power law having an index of 0.43 ± 0.09 over the range -4.7 to -3.6 in log (O/H). One possible interpretation of this trend is that the most metal-poor galaxies are the youngest and dominated by the products of early enrichment by massive stars, while more metal-rich galaxies show increasing, delayed contributions of carbon from intermediate-mass stars. However, recent evolution models for massive stars including mass loss suggest that the yield of carbon from massive stars may increase with metallicity relative to the yield of oxygen; new chemical evolution models for the solar neighborhood which include nucleosynthesis from these recent stellar evolution models predict a C/O abundance evolution similar to that observed in the metal-poor galaxies. The trend in the C/N ratio increases steadily with O/H in the irregular galaxies, but decreases suddenly for solar neighborhood stars and H II regions. This may indicate that the bulk of nitrogen production is decoupled from the synthesis of carbon in our Galaxy. Our results also suggest that it may not be appropriate to combine abundances in irregular galaxies with those in spiral galaxies to study the evolution of chemical abundances. Our measured C/O ratios in the most metal-poor galaxies are consistent with predictions of nucleosynthesis from massive stars for Weaver & Woosley's best estimate for the $^{12}C(\alpha, \gamma)^{16}O$ nuclear reaction rate, assuming negligible contamination from carbon produced in intermediate-mass stars in these galaxies.

We detect a weak N III] 1750 Å multiplet in SMC N88A and obtain interesting upper limits for two other objects. Our 2 σ upper limits on the 1750 Å feature indicate that the N^{+2}/O^{+2} ratios in these objects are not significantly larger than the N^{+}/O^{+} ratios measured from optical spectra. This behavior is consistent with predictions of photoionization models, although better detections of N III] are needed to confirm the results.

Subject headings: galaxies: abundances — galaxies: evolution — H II regions — ultraviolet: galaxies

1. INTRODUCTION

The evolution of the relative abundances of the chemical elements provides clues to the star-formation history and evolution of a galaxy (Wheeler, Sneden, & Truran 1990). Carbon and oxygen are among the most important in this regard, and knowledge of the variation of their abundances is important for a variety of problems, including (1) C and O constitute the bulk of the matter that is not hydrogen or helium, and thus are important sources of interior opacity in stars. Knowledge of the time evolution of C and O abundances is necessary to properly model the structure and evolution of stars at different ages; e.g., theoretical isochrones can give different ages for globular clusters for different values of O/Fe in the stars (VandenBerg 1985). (2) The formation of the CO molecule in the interstellar medium (ISM) should be regulated by the relative abundances of C and O at some level, so an understanding of the variation of C/H and C/O in the ISM is relevant for modeling the formation of CO molecules and the possible effects of abundance variations on the $I(CO)/N(H_2)$ relation. (3) There is evidence that the interstellar dust-to-gas ratio is related to the interstellar carbon abundance (Mathis 1990), so knowledge of C (and also Si) abundances in a variety of environments is relevant to understanding the amount, composition, and evolution of dust in those environments. (4) In

[1] Based on observations with the NASA/ESA *Hubble Space Telescope* obtained at the Space Telescope Science Institute, which is operated by Association of Universities for Research in Astronomy, Inc., under NASA contract NAS 5-26555.

[2] Hubble Fellow.

theory, oxygen is synthesized almost entirely in massive stars ($M > 10\ M_\odot$), while carbon is produced in both massive and intermediate-mass stars. Thus, the ejection of some carbon is delayed in time with respect to oxygen, so the C/O ratio offers a potential "clock" for determining the relative ages of stellar systems. (5) Steigman, Gallagher, & Schramm (1989) have argued that the C abundance is a better measure of stellar He production than O, and therefore that it is better to compare He/H with C/H when extrapolating to the primordial He abundance. Few observations of C abundances are available to test this controversial hypothesis.

The primary obstacle to our understanding the evolution of carbon in other galaxies is the severe lack of high-quality measurements of carbon abundances. C has no strong, easily observable transitions in the optical; the most important species, C III, has emission lines of reasonable strength only in the UV (C III] 1907, 1909 Å), requiring spacecraft observations, while [C II] has observable transitions only in the UV (2324–2329 Å) and far-infrared. Considerable observational effort has been made attempting to measure C abundances and C/O ratios within H II regions in our own and other galaxies, from ground-based optical spectra and UV spectra from *IUE* (a brief list of references includes Torres-Peimbert, Peimbert, & Daltabuit 1980; Peimbert, Peña, & Torres-Peimbert 1986; Dufour, Schiffer, & Shields 1984; 1988; Dufour, Garnett, & Shields; Skillman 1991; Walter, Dufour, & Hester 1992; and Peimbert, Torres-Peimbert, & Dufour 1993). Useful observations of C lines in about a dozen H II regions have been obtained with *IUE*, but for most of these the C line detections are marginal. There are also large uncertainties associated with relating the UV spectrum to the optical lines due to corrections for reddening and for differences in aperture sizes for the optical and the UV observations (Dufour & Hester 1990). Hence, a typical carbon abundance measurement from *IUE* observations is uncertain by at least a factor of 2–3. In nearly all cases, improved measurements of the C lines are desirable.

We can overcome many of these uncertainties by observing collisionally excited UV emission lines from C^{+2} and O^{+2} simultaneously. *IUE* did not have the sensitivity necessary to measure O III] λ1666 except in high-excitation planetary nebulae. Therefore, we began a program of observations with the FOS on the *HST* of the intercombination doublets O III] 1661–1666 Å and C III] 1906–1909 Å in giant H II regions in a sample of dwarf emission-line galaxies to determine the general behavior of the C/O ratio at low metallicities. We report on the results of that program here.

2. OBSERVATIONS AND ANALYSIS

2.1. *HST Observations*

We obtained UV spectra of metal-poor dwarf emission-line galaxies with the FOS on *HST* during cycles 2 and 3. A journal of the observations and the *HST* observation identifications are given in Table 1. Most of the spectra were taken with grating G190H and the 1″ circular aperture (aperture B-3) to achieve 3 Å spectral resolution over the wavelength range 1600–2300 Å. This range includes important nebular emission features from C^{+2} (1907, 1909 Å) and O^{+2} (1661, 1666 Å), as wellas N^{+2} (1748–1754 Å) and Si^{+2} (1882, 1892 Å). Our integrations were chosen to be long enough to detect both the O III] and C III] features to 4 σ or better; C III] is typically much stronger than O III] in H II regions, so the S/N in O III] is the limiting factor in the accuracy of our results. This observational approach has many advantages over previous studies which combined UV data from *IUE* with ground-based data:

1. Measuring O III] and C III] together eliminates observational difficulties in combining ground- and space-based spectra, such as mismatched apertures and positioning uncertainties.
2. The interstellar extinction curve is nearly flat over the short-wavelength range 1600–2000 Å. Thus, the relative line strengths suffer very little from uncertainties due to reddening.
3. The UV O III] and C III] lines have similar excitation potentials, so that uncertainties in T_e have only a minor effect on the derived ionic abundances.
4. O^{+2} and C^{+2} also have similar ionization potentials, and so corrections for nebular ionization structure are also relatively small.

TABLE 1

JOURNAL OF FOS OBSERVATIONS

Object	Observation ID	Integration Time	Aperture
30 Doradus	Y1470202T	1800 s	B-3
	Y1470203T	1800 s	B-3
C1543+091	Y1470802T	1800 s	B-3
	Y1470803T	1800 s	B-3
	Y1470804T	1800 s	B-3
T1214−277	Y1470702T	1800 s	B-3
	Y1470703T	1800 s	B-3
	Y1470704T	1800 s	B-3
NGC 2363	Y1LL0102T	2100 s	C-1
	Y1LL0103T	1200 s	C-1
SBS 0335−052	Y1470102T	1800 s	B-3
	Y1470103T	1800 s	B-3
	Y1470104T	1800 s	B-3
I Zw 18	Y1470502M	1650 s	B-3
	Y1470503M	1650 s	B-3
SMC N88A	Y1M70302T	1200 s	C-4

One observation, that of NGC 2363, was taken with G190H as well, but through the 1″ square paired aperture (aperture C-1). This sampled two regions of the nebula separated by 3″ Only one of the positions had sufficient signal-noise to be useful for our abundance determinations, and we present results for that position only. Finally, for the H II region N88A in the SMC we use a spectrum taken through the 0.″7 × 2.″0-BAR aperture (aperture C-4), centered on the ionizing star.

The target objects (typically bright H II regions located in low surface brightness galaxies) were positioned in the spectrograph aperture by first centering on a nearby star ($< 1'$) using a binary acquisition, then transferring to the target via blind offset. Following each spectroscopic observation we obtained a short white-light image through the 4.″3 target acquisition aperture to check the positioning. In two cases (I Zw 18 and T1214−277) the aperture missed the strong emission-line peak by $\sim 1''$ and sampled a lower surface brightness region instead, resulting in lower signal-to-noise in those spectra. We did obtain a weak detection of O III] in T1214−277, but only an upper limit for O III] in I Zw 18. For all of the observations for the other targets, the acquisition images showed that the spectrograph aperture was at the correct position.

The spectra were processed through the standard *HST* pipeline reductions, with corrections for flat-fielding, wavelength determination, instrumental background subtraction, and photometric calibration. The instrumental and sky background are negligible for our observations; our objects are bright in the UV compared to the background, and there are

no significant geocoronal emission lines in the wavelength region of interest. For the NGC 2363 observation we suppressed the sky subtraction option and simply summed the total spectrum at each position. There is no direct photometric calibration for the C-1 aperture. However, our scientific analysis requires accurate relative spectrophotometry only, and since the different FOS apertures should not introduce systematic color errors in the flux calibration, we used the (then current) calibration for the B-3 aperture scaled by the difference in aperture size. As a result, the absolute fluxes for NGC 2363 may not be accurate. Examples of our FOS spectra are shown in Figure 1.

Line fluxes were measured by direct integration under the line profiles and by fitting Gaussian profiles to the lines. Both methods gave very good agreement for lines with high signal/noise. Our measured line fluxes are listed in Table 2. The uncertainties in the line fluxes were determined from the statistical noise over the wavelength interval of each line (determined by the FWZI) combined with the uncertainty in the relative spectrophotometry of the FOS, which is less than 5% (R. C. Bohlin, private communication). Our 1 σ uncertainties in the line strengths computed in this way are listed in Table 2.

TABLE 2

LINE INTENSITIES FROM FOS OBSERVATIONS

Object	O III] λ1666	N III] λ1750	C III] λ1909
Fluxes in 10^{-15} ergs cm^{-2} s^{-1}			
30 Doradus.....	1.22 ± 0.95	<1.3	12.05 ± 0.32
C1543+091	3.35 ± 0.73	<1.3	9.80 ± 0.32
T1214−277	0.46 ± 0.35	<0.5	1.18 ± 0.13
NGC 2363.....	13.3 ± 2.2	<5.1	57.7 ± 1.3
SBS 0335−052.....	3.22 ± 0.98	<1.6	5.79 ± 0.47
I Zw 18	<2.9	<1.7	2.40 ± 0.41
SMC N88A	19.5 ± 1.4	3.2 ± 2.1	106.0 ± 5.6
Line Strengths Normalized to $I(\lambda 1909)$			
30 Doradus.....	0.10 ± 0.08	<0.01	1.00
C1543+091	0.34 ± 0.08	<0.13	1.00
T1214−277	0.39 ± 0.31	<0.40	1.00
NGC 2363.....	0.23 ± 0.04	<0.09	1.00
SBS 0335−052.....	0.56 ± 0.18	<0.28	1.00
I Zw 18	<1.2	<0.70	1.00
SMC N88A	0.27 ± 0.03	0.03 ± 0.02	1.00

2.2. *Supporting Optical Observations*

For our targets there exist excellent ground-based optical spectra, either published or in preparation for publication. The optical spectra can be found in Campbell, Terlevich, & Melnick (1986) for C1543+091; Pagel et al. (1992) for T1214−277; Skillman & Kennicutt (1993) for I Zw 18; Gonzalez-Delgado et al. (1994) for NGC 2363; Mathis, Chu, & Peterson (1985) for 30 Doradus; Terlevich et al. (in preparation) for SBS 0335−052; and Dufour et al. (in preparation) for N88A. From the optical spectra we obtain physical parameters needed to complete the analysis of the UV spectra: interstellar reddening electron temperature T_e, electron density n_e, abundances for oxygen and other heavy elements, and the degree of ionization of the nebular gas, measured by O^{+2}/O.

We use the normal interstellar extinction law of Seaton (1979) to estimate the reddening correction based upon the measured extinction values from our optical spectra. The difference in reddening between 1650 Å and 1910 Å is only 0.023 dex for $A_V = 1$ mag, or less than 5%. Except for 30 Doradus, our estimated reddenings are well under 1 mag visual, and so

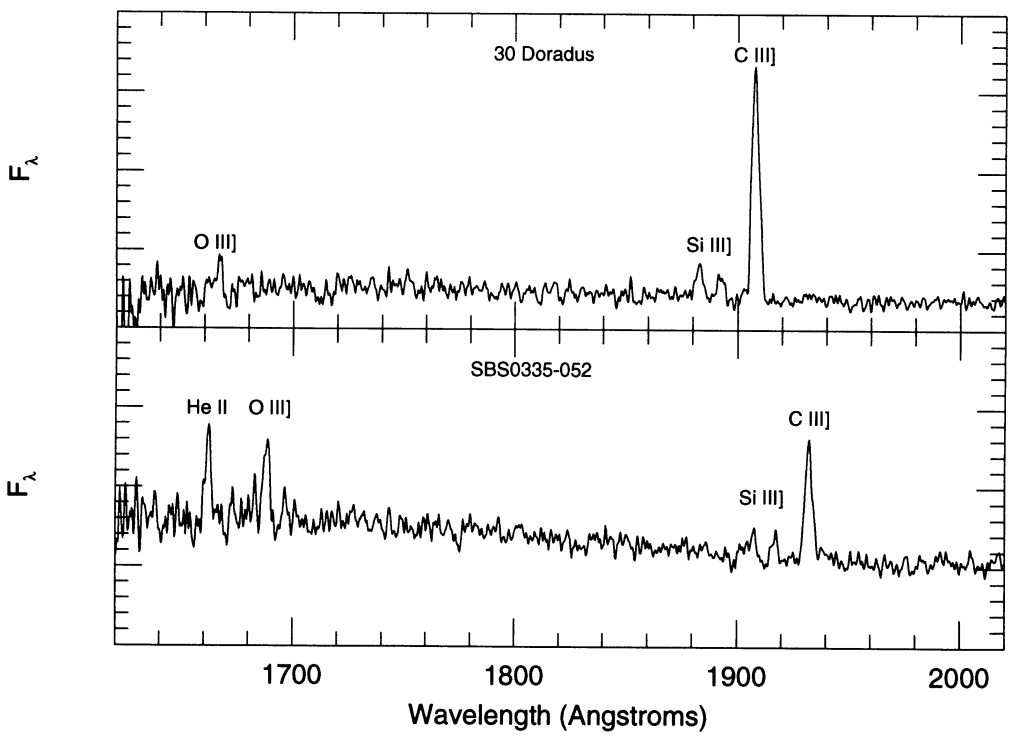

FIG. 1.—FOS spectra of two giant extragalactic H II regions, showing the O III] 1666 Å, Si III] 1883, 1892 Å, and C III] 1908 Å features. *Top*: 30 Doradus; *bottom*: SBS 0335−052. Both spectra have been smoothed with a three-point Gaussian filter.

TABLE 3

C/O ABUNDANCE RATIOS FROM FOS OBSERVATIONS

Object	30 Dor	SMC N88A	NGC 2363	C1543+091	T1214−277	SBS 0335−052	I Zw 18
log O/H	−3.70 ± 0.10	−3.91 ± 0.04	−4.08 ± 0.04	−4.24 ± 0.10	−4.41 ± 0.05	−4.64 ± 0.06	−4.83 ± 0.04
T_e	10,400 ± 400	14,000 ± 500	14,800 ± 500	16,100 ± 500	17,800 ± 800	19,500 ± 800	19,600 ± 900
C^{+2}/O^{+2}	0.31 ± 0.25	0.15 ± 0.02	0.18 ± 0.04	0.13 ± 0.04	0.12 ± 0.10	0.087 ± 0.035	>0.04
$X(O^{+2})$	0.83	0.96	0.94	0.90	0.95	0.91	0.84
ICF	1.06 ± 0.14	1.33 ± 0.48	1.31 ± 0.45	1.20 ± 0.30	1.32 ± 0.45	1.21 ± 0.31	1.09 ± 0.15
log C/O	−0.48 ± 0.26	−0.72 ± 0.17	−0.63 ± 0.15	−0.81 ± 0.15	−0.80 ± 0.28	−0.94 ± 0.17	>−1.35
N^{+2}/O^{+2}	<0.10	0.016 ± 0.011	<0.04	<0.04	<0.12	<0.06	...

interstellar reddening does not seriously affect the observed relative strengths of C III] and O III]. For N88A the bulk of the observed extinction is local to the SMC, and in this case we use the SMC extinction law of Prevot et al. (1984) to correct the relative strengths of the UV lines. The corrected UV line strengths normalized to C III] are listed in Table 2.

3. IONIC AND ELEMENTAL ABUNDANCE

3.1. *Physical Conditions*

From the optical measurements listed in § 2.2 we obtain estimates of the electron temperatures (from the [O III] lines) and electron densities (from the [S II] lines) in our FOS target H II regions. The measured electron temperatures are listed in Table 3; the densities in these objects ($<10^3$ cm^{-3}) are too small for significant deactivation of the UV transitions we observe. Our FOS position in 30 Doradus is located on the bright knot between positions III-2 and III-3 from Mathis et al. (1985); we used an average of the derived physical parameters and abundances at those two positions to analyze our FOS spectrum.

3.2. *Ionic Abundances*

Our analysis is relatively straightforward. The electron densities for our H II regions are all well below the critical densities for collisional de-excitation of the C III] and O III] intercombination lines. Therefore, we can compute the C^{+2}/O^{+2} abundance ratio in the low-density limit, as demonstrated in Aller (1984, chap. 5). and Osterbrock (1989, chap. 5). In the low-density limit, the emission-rate coefficient for a collisionally excited emission line is given by

$$j(\lambda) = h\nu \frac{8.629 \times 10^{-6}}{T_e^{0.5}} \frac{\Omega(1,2)}{\omega_1} \exp\left(\frac{-\chi}{kT_e}\right) N_e N(X^{+i}) , \quad (1)$$

where T_e and N_e are the electron temperature and density, $\Omega(1, 2)$ is the effective collision strength between the two levels, ω_1 is the statistical weight of the lower level, χ is the excitation potential of the transition, and $N(X^{+i})$ is the number density of the ion under consideration.

The main useful sources of effective collision strengths for C III ^3P–$^1S^o$ at electron temperatures below 20,000 K are Mendoza (1983) (based upon the computations of Dufton et al. 1978 and Berrington et al. 1977 plus data from the Daresbury atomic database), and Berrington (1985). Berrington does not provide collision strengths below log $T_e = 4.1$, but the collision strength for ^3P–$^1S^o$ is nearly constant between 10,000 K and 20,000 K, suggesting reliable extrapolation is possible. Mendoza's collision strengths are only 4%–5% smaller than Berrington's, and here we adopt the mean values from the two papers. Nevertheless, new calculations of C III collision strengths over the full range of nebular temperature conditions are desirable.

For O III $^5S^o$–^3P (from which the λ1661, 1666 transitions arise) there are several similar, independent calculations (Baluja, Burke, & Kingston 1981 [BBK]; Aggarwal 1983 [A83], and Burke, Lennon, & Seaton 1989 [BLS]). Comparing the three calculations, we see that BLS and A83 find similar values for Ω as a function of T_e, while the values from BBK are smaller by 6%–8%. On the other hand, for $\Omega(^1D$–$^3P)$ BLS obtain values higher than BBK and A83 by about the same amount, while for ^1S–^1D the three calculations give Ω's spread out approximately evenly over a range of about 7%. It may be that this range reflects the intrinsic precision of the current electron impact calculations. Since this spread is small compared with other uncertainties in our analysis, we take the mean of the collision strength values from BBK, A83, and BLS for our abundance calculations, with the adopted uncertainty of ±5%. The collision strength values we adopt for three different temperatures are listed in Table 4.

With these values for the C III and O III collision strengths the C^{+2}/O^{+2} ionic abundance ratio can be computed directly from the C III]/O III] line ratio by using equation (1) to derive the relation

$$\frac{C^{+2}}{O^{+2}} = 0.089 e^{-1.09/t} \frac{I(\lambda 1909)}{I(\lambda 1666)} , \quad (2)$$

where $t = T_e/10^4$ K and $I(\lambda)$ is the line intensity. The numerical coefficient before the exponential has a small temperature dependence, varying by 6% over the range 10,000–20,000 K, with the average value shown in equation (2). All of the H II regions in our sample have electron temperatures within this range. Our computed C^{+2}/O^{+2} ratios are listed in Table 3. In these calculations we have assumed that our measured [O III] electron temperatures are appropriate for both C III] and O III]. This is a reasonable assumption given that the C III] and O III] lines are similar in both ionization and excitation. In addition, Garnett (1992) compared characteristic ion-weighted electron temperatures for various ions using photoionization

TABLE 4

ADOPTED O III ^5S–^3P COLLISION STRENGTH

T_e (K)	$\Omega(^5S$–$^3P)$
10,000.....	1.235
15,000.....	1.284
20,000.....	1.295

modeling, and found little systematic variation of T(C III) with respect to T(O III).

Despite the lack of detections of the N III] λ1750 multiplet, we can estimate upper limits on N^{+2}/O^{+2} in a similar way to C^{+2}/O^{+2}. The relation is

$$\frac{N^{+2}}{O^{+2}} = 0.212e^{-0.43/t}\frac{I(\lambda 1750)}{I(\lambda 1666)}, \quad (3)$$

using the collision strengths for N III computed very recently by Blum & Pradhan (1992). Our 2 σ upper limits, determined over a 10 Å bandpass, are listed in Table 3. We did obtain a weak detection of N III] in N88A, and we list the computed N^{+2}/O^{+2} ratio based on that detection in Table 3.

3.3. *Corrections for Ionization*

To first order, one can say that C^{+2} and O^{+2} are similar ionization states, and therefore that $C^{+2}/O^{+2} \approx$ C/O. However, the various ions of C and O have different ionization potentials: for C^{+} and C^{+2}, the IPs are 24.4 eV and 47.9 eV, respectively, while for O^{+} and O^{+2} the IPs are 35.1 and 54.9 eV. Thus, we might expect nonnegligible amounts of C^{+3} in H II regions ionized by the hottest O stars, while in nebulae ionized by cooler stars the fraction of carbon in C^{+2} may exceed the O^{+2} fraction. The relative ionization of these species can vary systematically if, for example, stellar ionizing continua vary with metallicity, the stellar mass–$T_{\rm eff}$ relation varies with metallicity (Maeder 1990), or if the stellar mass function varies with metallicity (Terlevich & Melnick 1985). Therefore, we must look at photoionization models to estimate the corrections for ionization to convert our measured C^{+2}/O^{+2} ratios to true C/O abundance ratios.

To look at this we have computed photoionization models using the code described in Shields et al. (1981) and Garnett (1989). The model nebulae were computed as dust-free spherical nebulae consisting of filaments in a vacuum with some filling factor ϵ. We constructed ionizing continua for OB associations in a manner similar to that employed by McGaugh (1991). We used stellar mass–effective temperature relations at metallicities $Z = 0.001$, 0.004, and 0.008 from the stellar evolution models of Schaller et al. (1992), Schaerer et al. (1993a, b), and Charbonnel et al. (1993) for both ZAMS and 2 Myr old stars. Lyman-continuum luminosities as a function of stellar mass were then determined from the $T_{\rm eff}$–N(Lyc) relation of Panagia (1973) for the ZAMS; for 2 Myr old stars, we scaled N(Lyc) from the ZAMS value as the bolometric luminosity. A Salpeter initial mass function over the range 10–100 solar masses was used to determine the relative contribution of a given stellar mass to the total ionizing luminosity of the cluster. Stellar fluxes from the non-LTE models of Mihalas (1972) determined the shape of the ionizing continua.

The nebula models were computed for the same metallicities as the stellar evolution models, i.e., $Z = 0.001$, 0.004, and 0.008. The models included the elements H, He, C, N, O, Ne, Mg, Si, S, and Ar. With the following exceptions, the elements heavier than H were kept in their solar system ratios.

1. We took N/O = 0.03, the average value observed in metal-poor irregular galaxies (Garnett 1990).

2. Mg/O and Si/O were reduced by a factor of 10 from their solar system ratios to simulate depletion of Mg and Si onto grains.

3. The He mass fraction Y was varied as $Y = 0.23 + 5\,\Delta$(O/H).

In computing the models the number of ionizing photons was kept fixed at log N(Lyc) = 52.0 photons s^{-1} while the ionization parameter U (as defined in Shields & Searle 1978) was varied by adjusting the gas filling factor. The models cover the range $-3.0 < \log U < -2.0$, the typical range for giant H II regions (Shields 1990).

The results from the models are displayed in Figure 2, where we plot the ratio of the C^{+2} and O^{+2} volume fractions, $X(C^{+2})/X(O^{+2})$, versus the O^{+2} fraction $X(O^{+2})$. In terms of the ionic abundance ratio C^{+2}/O^{+2}, the elemental abundance ratio C/O is then

$$\frac{C}{O} = \frac{C^{+2}}{O^{+2}}\left[\frac{X(C^{+2})}{X(O^{+2})}\right]^{-1} = \frac{C^{+2}}{O^{+2}} \times \mathrm{ICF}, \quad (4)$$

where ICF refers to the "ionization correction factor." For comparison, we also plot in Figure 2 the results from the model grid of Stasińska (1990) for single stars with $T_{\rm eff}$ from 35,000 K to 55,000 K. Notice that the model points fall within a well-defined band in the diagram, with the spread in the band increasing as the fraction of O^{+2} increases (toward the left), as well as the good agreement between our models for OB clusters and those of Stasińska for single values of $T_{\rm eff}$. The spread in $X(O^{+2})$ reflects mainly the effects of changing the ionization parameter in the models. At the same time, the spread in $X(C^{+2})/X(O^{+2})$ reflects mainly changes in the hardness of the ionizing radiation: for cooler stars (or, equivalently, an older cluster), the bound-free absorption edges in the stellar atmospheres are stronger, resulting in fewer photons capable of ionizing C to C^{+3}. Thus, in the case of a nebula with high ionization parameter but relatively cool stars, essentially all of the C and O are twice ionized.

For the H II regions we have observed, $X(O^{+2})$ has been measured from the optical spectra, and is listed in Table 3. Therefore, we can estimate the correction for unobserved ions of carbon directly from Figure 2. For our measured values of $X(O^{+2})$, we find the mean value of $X(C^{+2})/X(O^{+2})$ from the diagram; the correction from the observed C^{+2}/O^{+2} to C/O is then given by equation (4). The uncertainty in that correction is determined by the spread in $X(C^{+2})/X(O^{+2})$ at fixed $X(O^{+2})$. The correction factors (ICFs) derived for our objects are listed in Table 3 along with their uncertainties, as well as the final values of the C/O abundance ratios in our objects.

3.4. *Uncertainties*

The dominant sources of uncertainty in our abundance determinations are the finite S/N in our O III] line measurements and the uncertainty in the ICF. The uncertainties in the line strengths listed in Table 2 were determined from the statistical noise in the spectra over the FWZI for each measured line combined in quadrature with the uncertainty in the relative spectrophotometry of the FOS, as discussed in § 2.1. We take the uncertainty in the ICF to be the full range in $X(C^{+2})/X(O^{+2})$ corresponding to each observed value of $X(O^{+2})$, as determined from Figure 2. Uncertainties in the electron temperature contribute to the error in the abundance ratio through the exponential term in equation (2); the weak dependence of C^{+2}/O^{+2} on T_e means that uncertainties of less than 1000 K in T_e have only a small effect on the abundance ratio, less than 10%. Errors due to uncertainty in the reddening

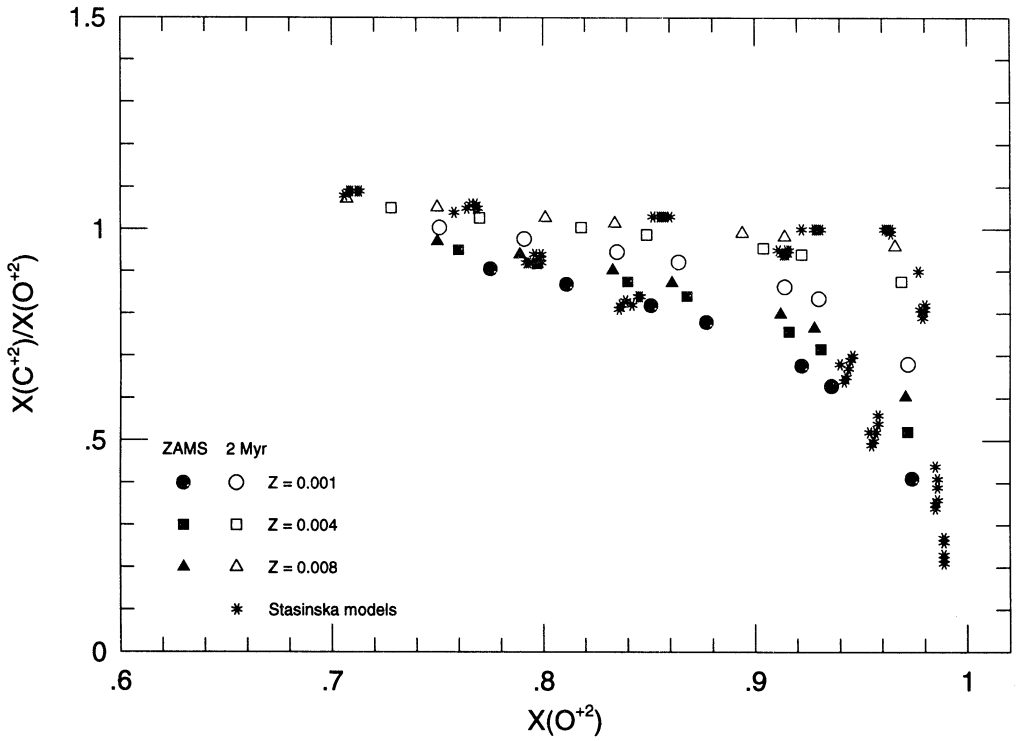

FIG. 2.—The ionization of C^{+2} and O^{+2} in H II region models, as described in the text. $X(C^{+2})$ and $X(O^{+2})$ are the fractions of C and O in the doubly ionized state. $[X(C^{+2})/X(O^{+2})]^{-1}$ is the correction (ICF) to convert C^{+2}/O^{+2} into C/O.

correction are less than 2% for all of our objects. Uncertainties in the collision strengths introduce approximately 8% uncertainty in the C/O abundance ratio, neglecting possible systematic errors in the quantum calculations.

There is some concern that the imprecise position of the spectrograph for I Zw 18 and T1214−277 could lead to errors in physical conditions and hence in the C/O ratios. The most likely effect of the displacement is that the data come from regions with slightly lower ionization and/or electron temperature. Both effects would mean our derived C/O ratios are artificially enhanced compared to the true values. Lower intrinsic C/O ratios in these two galaxies would reinforce the trends we observe.

4. DISCUSSION

4.1. *Trends in Relative Abundances*

The resulting carbon and oxygen abundances for the targets from our sample are displayed in Figure 3, plotted as log (C/O) versus log (O/H). We also plot for comparison the values for the solar system (Grevesse & Noels 1993), and the mean abundances in B stars from Gies & Lambert (1992, GL92) and Cunha & Lambert (1994, CL94), as well as the abundances for the Orion Nebula (mean of four studies listed in CL94), and NGC 2363 (Peimbert et al. 1986). The latter point is based on a detection of O III] 1661–1666 Å in both high-dispersion and low-dispersion *IUE* spectra; note the good agreement between our results for NGC 2363 and those from the *IUE* data. The following discussion is based solely on those points for which we have O III] detections, i.e., excluding the lower limit for I Zw 18.

The data show an apparently continuous increase in C/O with increasing O/H in these metal-poor systems; the behavior of log (C/O) versus log (O/H) is consistent with a power law with slope 0.43 ± 0.09 (least-squares fit to the six FOS points, excluding I Zw 18). A formal fit gives

$$\log (\mathrm{C/O}) = A + B \log (\mathrm{O/H}) , \qquad (5)$$

where $A = 1.07 \pm 0.39$ and $B = 0.43 \pm 0.09$. Note that this fit applies only to the abundance range log O/H = −4.7 to log O/H = −3.6. By comparison, a simple chemical evolution model with instantaneous recycling predicts C/O = constant if both C and O are primary elements, or C/O ∝ O/H if O is primary and C secondary. Since only primary sources of C are known to exist, the trend in Figure 3 suggests that either (or both) the instantaneous recycling approximation does not hold for both C and O or that the yield of C varies with respect to O.

Figure 4 shows the variation of C/N with O/H, with nitrogen abundances obtained from the sources of optical spectra listed above. There is significantly greater scatter in this diagram. If we exclude the point for I Zw 18, it is difficult to discern a correlation between C/N and O/H. If we exclude the Orion and solar system points as well, then a trend of increasing C/N with O/H is apparent. Such a trend contrasts with the results for C/N from *IUE* and optical spectra, compiled and presented by Pagel (1985), which indicated that C/N is uncorrelated with O/H. A larger sample of galaxies observed with the FOS is needed to confirm and delineate the trend more clearly.

Figure 5 presents a comparison of our new results with previous results found in the literature. Here we are interested in two questions: (1) do these new results agree with previous results on C/O measurements of H II regions in dwarf galaxies and (2) is the pattern of C/O versus O/H seen in the dwarf galaxies similar to that seen in our Galaxy?

The top panel of Figure 5 addresses the first question. Here we have plotted the points from Figure 3 along with results

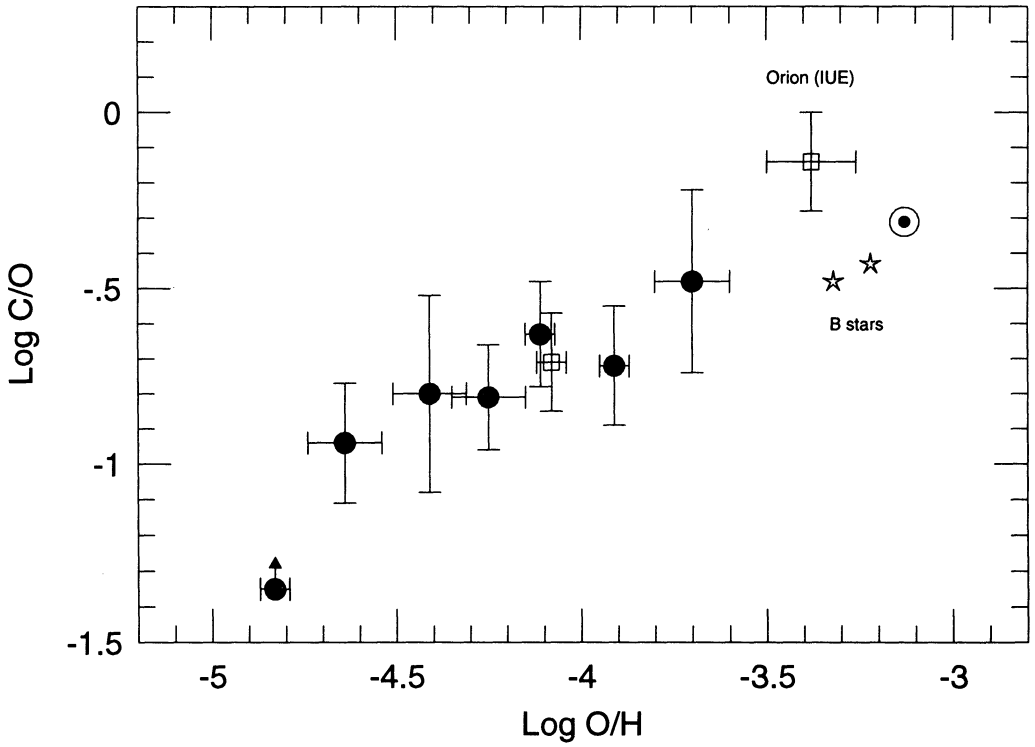

FIG. 3.—The C/O abundance ratio in irregular galaxies vs. O/H. Filled circles are the data from our FOS spectra; unfilled squares are data for Orion and NGC 2363 obtained from *IUE* spectra. The stars represent the mean abundances in B stars determined by GL92 and CL94.

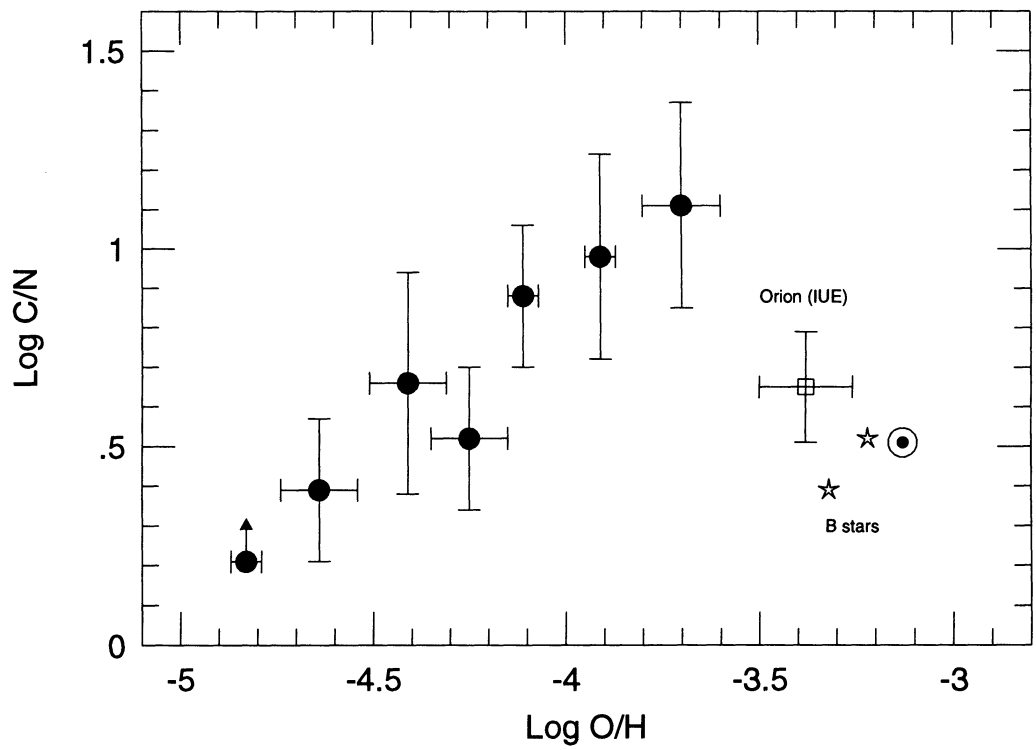

FIG. 4.—C/N abundance ratio vs. O/H in irregular galaxies. Symbols are the same as in Fig. 3.

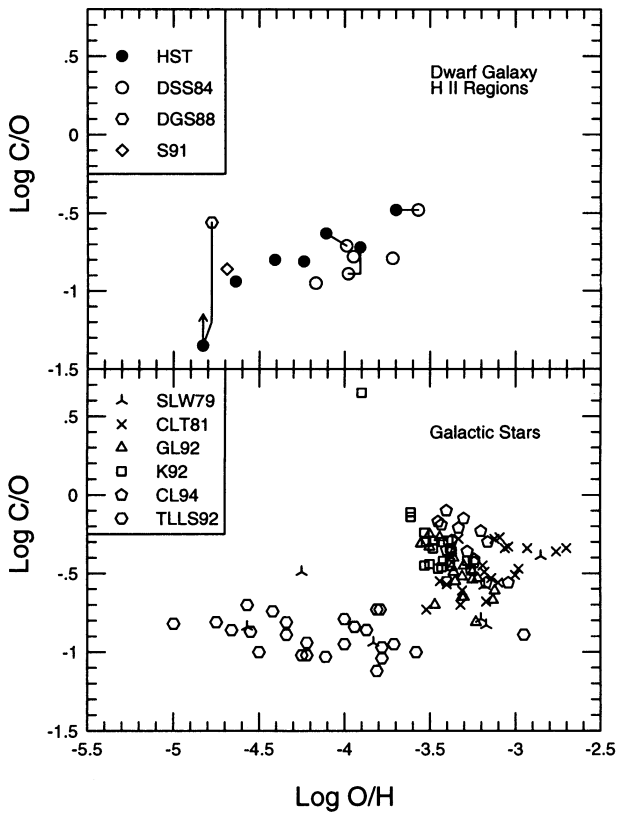

FIG. 5.—The C/O abundance ratio vs. O/H for H II regions in irregular galaxies and Galactic stars. In the top figure the new *HST* results are plotted with previous results from *IUE* observations. In the lower figure observations of Galactic stars are presented. The symbols are described in the text.

from *IUE* observations taken from the literature. The open circles come from Dufour, Schiffer, & Shields (1984, DSS84), the open hexagon represents I Zw 18 as from Dufour, Garnett, & Shields (1988, DGS88) as adjusted by Dufour & Hester (1989), and the open diamond represents UGC 4483 as reported by Skillman (1991, S91). Points which represent observations of the same galaxy are connected. The abundances are taken directly from the literature and are not recalculated from original line strengths (since, in some cases, the line strengths are not reported). As noted earlier for NGC 2363, there is reasonably good agreement between the *IUE* measurements and the *HST* measurements for those objects which have both measurements. Our new results and those of previous studies clearly indicate a need for new, deep FOS spectra of I Zw 18 and H II regions in the Milky Way and other spiral galaxies to extend the trend of C/O to metallicities outside the range of our present sample.

The bottom panel of Figure 5 presents C/O and O/H measurements of Galactic stars taken from the literature. The data are taken from Sneden, Lambert, & Whitaker (1979, SLW79), Clegg, Lambert, & Tomkin (1981, CLT81), Gies & Lambert (1992, GL92), Kilian (1992, K92), Tomkin et al. (1992, TLLS92), and Cunha & Lambert (1994, CL94). There is considerable scatter in log (C/O) for the disk stars, with an average value of about -0.4. For the halo stars, log (C/O) is fairly constant at -0.9 (with a scatter consistent with observational errors). If the trend of increasing C/O with O/H seen in the H II regions of dwarf galaxies is supported by more observations, then a clear difference is emerging between the abundance pattern seen in our Galaxy and the dwarf galaxies. The possible origins of such differences are discussed in § 4.5.

In the highly ionized nebulae comprising our sample, the singly ionized species (O^+, N^+, etc.) represent only a small fraction of the total abundance of the various elements in the gas. This has been a particularly severe problem for nitrogen since only N^+ is observable in the visual spectrum. Measurements of far-IR fine structure lines of [N III] and [O III] have been made by Lester et al. (1987), among others, to study the variation of N/O in H II regions and to compare with optical measurements of N^+/O^+. They found that N^{+2}/O^{+2} exhibited a radial gradient across the Galaxy, whereas N^+/O^+ from optical spectra did not. Garnett (1990) showed that ionization effects could be very important in interpreting such trends, and that measurements of both N^{+2} and N^+ are needed to determine N/O with certainty. Unfortunately, the IR and optical samples of N/O measurements have little overlap, so the true evolution of N/O is still controversial.

One can also look at the UV lines of N III] near 1750 Å to measure N^{+2} in hot H II regions. The lines are very weak and require long exposures to obtain a good detection; our exposures were not long enough to obtain more than upper limits on the N III] intensities. However, for three of our objects (N88A, NGC 2363, and C1543+091—Table 4), the 2 σ upper limits on N^{+2} are low enough to indicate that N^{+2}/O^{+2} is not significantly larger than N^+/O^+ from optical observations. This is consistent with the photoionization models for metal-poor nebulae by Garnett (1990), who suggested that optical measurements of N^+ alone can provide reliable measurements of the nitrogen abundances in such objects. This provides some confidence that our C/N ratios are reliable. Nevertheless, longer integrations of the brightest objects are needed to obtain good measurements of N III] and confirm this hypothesis.

4.2. *Depletion onto Grains*

Observations of interstellar extinction and line absorption demonstrate the need to consider depletion of heavy elements (including carbon and oxygen) onto grains in order to derive accurate elemental abundances in the ISM. For our analysis we need to examine how much depletion of carbon and oxygen is appropriate for our H II regions and the possible effect on the observed trend in the gas-phase C/O ratio. Much of the discussion below is based on information from Tielens & Allamandola (1987), Jenkins (1987), and Mathis (1990).

Theoretical arguments suggest that there should be little (0.1–0.2 dex) depletion of O onto grains in the diffuse ISM (Meyer 1985; Tielens & Allamandola 1987). Greater depletions are expected from the buildup of icy mantles (mainly water ice) on grains within dense molecular clouds, but these mantles are not expected to survive the harsher conditions of the diffuse ISM. On the other hand, observations of interstellar absorption lines from O show depletions of approximately 0.4 dex (Jenkins 1987), with no discernible trend with the cloud density. The amount of depletion inferred, however, depends on the reference abundances used. Typically, solar abundances have been used as the reference, yielding the above O depletion. More recently, GL92 and CL94 have determined abundances for B stars in the solar neighborhood and Orion; these studies indicate that the B-star oxygen abundances are systematically smaller than in the Sun, and in better agreement with the results from nearby H II regions. Sofia, Cardelli, & Savage (1994) have shown that using the average B-star abundance for

O as the reference standard leads to smaller derived depletions for O in the local ISM—approximately 0.2 dex.

The situation for carbon is even more uncertain. There are few reliable measurements of interstellar carbon lines, because the most easily observed lines are often highly saturated. Cardelli et al. (1993) and Sofia et al. (1994) discuss recent measurements of weak interstellar C II line measurements with the *HST*. The results for three sight lines, referenced to solar abundances, indicate a C depletion of about 0.4 dex also, although the lower depletion of C toward ξ Per suggests that carbon depletion may be variable; data for more sight lines are certainly needed to address this question. The inferred depletions are again strongly dependent on the choice of reference abundances; a comparison of the interstellar C abundances with the mean value for B stars from GL92 would lead one to infer little or no depletion of carbon (Sofia etal. 1994). Such a result would be difficult to understand. However, GL92 noted that the distribution of C abundances for their sample showed a tail toward low abundances, while the distribution of N abundances shows a tail toward higher abundances. This suggests that some of the stars may exhibit the signs of CN processing, and that the mean C abundance quoted by GL92 could underestimate the true mean of the original abundances. Indeed, Cunha & Lambert (1993) obtain a somewhat higher mean C abundance for their sample of B stars in Orion. Furthermore, the most recent compilation of solar abundances (Grevesse & Noels 1993) has resulted in a slight downward adjustment of the solar O/H by 0.06 dex. Using the CL94 abundances as reference alleviates the problem somewhat, although the inferred carbon depletion is still relatively small ($\approx$0.2 dex).

The uncertainties discussed above make it difficult to determine how to apply the depletion results to our measured abundances. Direct application of the above results leads to equal depletions of about 0.35 dex for C and O (based on solar reference abundances) or 0.15 dex for both (based on B star abundances). Applying these depletions changes the C and O abundances by equal factors, so the trend observed in Figure 3 would be unchanged, although the abscissa scale would shift to higher values. Similarly, the C/N ratios in Figure 4 would all change systematically (N shows little evidence for depletion in the ISM), but the trend in C/N with O/H would not change.

Another concern is that depletions may vary with metallicity. Unfortunately, there is little evidence for or against this possibility. Measurements of interstellar extinction curves appear to show that the interstellar dust-to-gas ratio [measured by $N_H/E(B-V)$] varies directly as the carbon abundance, and that the 2175 Å absorption feature (most commonly attributed to carbon-based compounds) weakens likewise. This *could* be interpreted as being consistent with a constant depletion of carbon with metallicity, but the uncertainties are large. Measurements of Si/O from our FOS spectra (Dufour et al., in preparation) also suggest that depletions do not vary significantly with metallicity. We can examine the effect on the observed abundance ratios by assuming the maximum possible variation. The worst case is for the depletions based on the solar reference abundances, i.e., 0.4 dex depletion for C and O at solar neighborhood metallicities. If the C depletion does not vary, but the O depletion decreases uniformly to zero for log O/H < -4.5, then such variation can account almost entirely for the trend in C/O in Figure 3, and the true trend would be that C/O is uncorrelated with O/H. (We reject the possibility that depletions can be *larger* at low metallicities.) On the other hand, Garnett (1990) has shown that the average N/O ratio in irregular galaxies is constant with O/H, based on zero depletion of oxygen. Since N is depleted very little in the ISM, an increasing O depletion with metallicity would lead to the conclusion that N/O *decreases* with metallicity in irregulars, a result very difficult to understand in the context of either nucleosynthesis or chemical evolution theory.

Another observation of possible relevance comes from the study of Calzetti, Kinney, & Storchi-Bergmann (1994). They have derived extragalactic extinction curves by comparing stellar continua of highly reddened and lightly reddened starburst galaxies. Remarkably, they note that their derived extinction laws show no evidence for the 2175 Å feature (after the galaxy spectra are corrected for Galactic extinction). Because of the large apertures they used and the high reddening toward many of their targets, scattering and optical depth effects could partly account for the Calzetti et al. result. On the other hand, Fitzpatrick (1985) has shown that stars in the region of 30 Doradus show weaker 2175 Å features than do stars in the LMC located far from 30 Doradus, while Rosa & Benvenuti (1995) find similarly weak 2175 Å features in FOS spectra of giant H II regions in M101. If the 2175 Å feature is indeed attributable to carbon-based grains, these results might indicate that such grains are destroyed in the energetic environment of a starburst, and thus that carbon depletions might be small in giant H II regions.

Given the uncertainties in depletions and the lack of information on their variation with metallicity, at the present time we choose to assume that grain depletions will not significantly affect the observed trends of C/O and C/N, although the abundance scales may change systematically.

4.3. *Nuclear Reaction Rates and C and O Yields*

^{16}O is predominantly a product of α-particle captures onto ^{12}C during the He-burning phase of stellar evolution. The amount of O ejected by a star depends on its mass—too small a star leaves its oxygen behind in the core remnant. Stellar evolution models generally show that 10 $M_\odot$ is the smallest star that can produce and eject new oxygen. ^{12}C is also produced during He burning through the well-known "triple-α" reaction. Theoretical models indicate that carbon can be ejected not only by massive stars, but also by intermediate-mass stars ($\approx$2–8 $M_\odot$) through the convective dredge-up of freshly synthesized carbon during the asymptotic giant branch evolution phase of these stars. Measurements of carbon abundances in planetary nebulae show that some of them have enrichments of carbon, confirming that dredge-up does occur in at least some intermediate-mass stars.

The relative amounts of C and O produced during He burning are sensitive to the nuclear reaction rate for the $^{12}C(\alpha, \gamma)^{16}O$ reaction, as demonstrated by the models of Weaver & Woosley (1993, hereafter WW93). The value of the cross section for this reaction has been a source of considerable uncertainty; details of the controversy are given in Rolfs & Rodney (1988). Some attempts have been made to determine the rate empirically. Arnett (1971), for instance, tried to constrain the reaction rate by comparing the solar system C/O ratio with the predictions of stellar nucleosynthesis. This kind of analysis assumed that both C and O are produced in massive stars only and that the C/O ratio does not evolve with time. Clearly, however, the observations of C/O in Galactic stars and extragalactic H II regions show that the C/O ratio has evolved. WW93 tried a similar approach to the problem, comparing their results for massive star nucleosynthesis with the

solar system abundance pattern, but *excluding* carbon in the comparison. They found that a reaction rate of 1.7 ± 0.5 times the Caughlan & Fowler (1988, hereafter CF88) rate produced the best match to the solar system abundance distribution for elements between O and Fe.

Recently, improved measurements of the $^{12}C(\alpha, \gamma)^{16}O$ cross section have been reported by Buchmann et al. (1993) and Zhao et al. (1993). The results represent improved agreement with each other compared with earlier measurements. Nevertheless, there is still significant disagreement in the measurements that requires resolution. In terms of the commonly used astrophysical S factor $S(E)$, Buchmann et al. measured a value $S_{E1}(0.3 \text{ MeV}) = 57 \pm 13$ keV-b, while Zhao et al. obtained a value $S_{E1}(0.3 \text{ MeV}) = 95 \pm 32$ keV-b for the same reaction. For comparison, WW93's best estimate corresponds to $S_{E1}(0.3 \text{ MeV}) = 102 \pm 30$ keV-b.

Here we attempt an independent estimate of the $^{12}C(\alpha, \gamma)^{16}O$ reaction rate by comparing the stellar nucleosynthesis results of WW93 with the C/O ratios measured in our most metal-poor galaxies. Figure 6 shows our observed C/O ratios overlaid with the C/O (by number) ratios obtained by integrating the WW93 results over the stellar mass range 11–42 $M_\odot$ with an IMF slope of −1.5 (taken from their Table 7); the calculations shown are for the case of "nominal" semiconvection as defined by WW93. The horizontal dotted lines show the theoretical integrated C/O ratios obtained for different values of the $^{12}C(\alpha, \gamma)^{16}O$ rate in units of the CF88 rate; each line is labeled with the value of the reaction rate used in the calculation.

Figure 6 shows that the observed C/O ratios in our three most metal-poor galaxies (not including I Zw 18) are consistent with WW93's estimate for $^{12}C(\alpha, \gamma)^{16}O$. However, our comparison depends on two important assumptions.

1. We assume that the most metal-poor galaxies in our sample have abundance ratios dominated by nucleosynthesis from massive stars. However, if intermediate-mass stars have contributed a significant amount of carbon in these galaxies, our observed C/O would require a larger $^{12}C(\alpha, \gamma)^{16}O$ rate. On the other hand, the WW93 models cover a mass range of only 11–40 $M_\odot$; more massive stars tend to produce relatively more oxygen and so a higher upper mass limit would drive the predictd C/O ratio down.

2. We also assume that the stellar initial mass function does not change significantly with metallicity. WW93 also provide nucleosynthesis results integrated over an IMF with a slope of −2.3; the integrated C/O ratio for this case is an average of only 11% larger than for slope −1.5, suggesting that the slope of the IMF does not affect abundance ratios significantly, within known uncertainties.

This comparison should be viewed with caution because of a number of additional uncertainties which can affect the results. First of all, we have only a small number of carbon measurements to work with at this point, and we cannot say with confidence yet that we know either the true variation of C/O with metallicity or the minimum value of C/O in these galaxies. Second, the final word on theoretical nucleosynthesis has certainly not been written yet. Convective treatments and stellar mass loss are still highly uncertain inputs to stellar evolution models and can have significant effects on the production of C and O. WW93 illustrate the effects of varying the convective treatment with a second set of stellar models with a reduced or

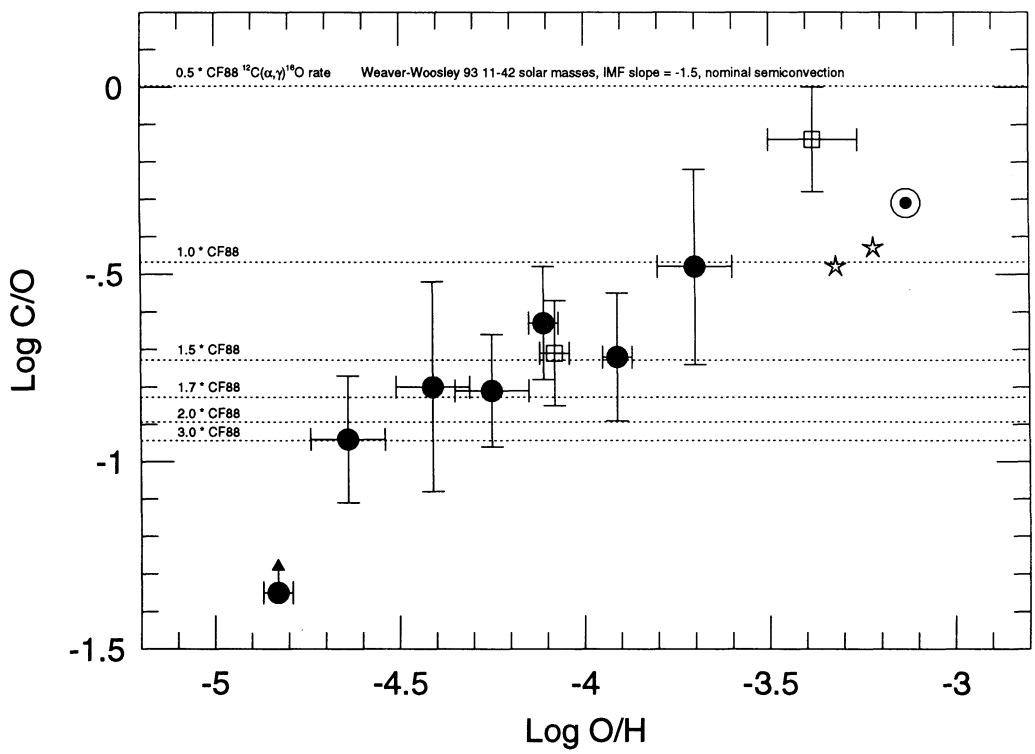

FIG. 6.—Comparison of our C/O abundance ratios in irregular galaxies with the results of stellar nucleosynthesis calculations (WW93). The horizontal dotted lines indicate the value of the C/O ratio one obtains by integrating the C and O produced by massive stars over a mass range 11–42 $M_\odot$ and an IMF with slope −1.5, for various values of the $^{12}C(\alpha, \gamma)^{16}O$ reaction rate. Each line is labeled with the magnitude of the reaction rate, as defined in WW93; the reaction rate increases from 0.5 times the CF88 rate for the top line to 3.0 times CF88 for the bottom line.

"restricted" semiconvection. These models result in integrated C/O ratios in ejected material up to twice as large as in the "nominal" semiconvection treatment. The effects of stellar mass loss (Maeder 1992; Woosley, Langer, & Weaver 1993) on stellar evolution and nucleosynthesis have only recently been explored extensively; we discuss some of the results below.

It is also apparent that more observations of C/O in metal-poor galaxies will be needed to clearly delineate the evolution of the C/O ratio and to define its lower bound. In particular, an improved measurement for I Zw 18 is a minimum requirement to anchor the low-abundance end.

4.4. *Chemical Evolution Concerns*

The firm result of this study is that the C/O abundance ratio in low-metallicity systems is lower than in the solar neighborhood, by up to a factor of 5 compared to the Sun, as illustrated in Figure 3. The low C/O ratios we observe in our most metal-poor galaxies are consistent with the C/O ratios observed by Reimers et al. (1992) in Lyman-limit and metal-line absorption systems toward the QSO HS 1700+6416. In seven absorption systems between redshifts 1.8 and 2.6, they measured C/O ratios ranging from 0.1 to 0.2. One lower redshift system, at $z = 1.1572$, showed a solar C/O ratio. These results combined with ours clearly show that the C/O ratio has evolved from low values at early times to the present-day "cosmic" ratio.

We begin our interpretation of the trend in Figure 3 within the framework of the simple "closed box" model of chemical evolution, in which a system evolves without gas flows into or out of the system, and in which stars are assumed to have a negligible lifetime, ejecting products of nucleosynthesis as soon as they are formed (the instantaneous recycling approximation). We also assume initially that the chemical yields for a generation of stars do not change with time or composition. Consideration of nucleosynthesis sites for carbon and oxygen indicate that both C and O should be so-called "primary" elements (that is, produced from material that was originally hydrogen or helium in the star); in such a case, the simple model predicts that C and O should vary in lockstep with a constant ratio. This prediction is clearly at odds with the observations.

There are several possible ways to explain the variation in C/O with O/H.

1. *Breakdown of the instantaneous recycling approximation.*—Stars do in fact have nonnegligible lifetimes. As a result, a temporal variation in the ratio of two elements will be observed if the two elements are produced in stars with different lifetimes (Tinsley 1979). It was noted earlier that carbon can be produced in both massive stars and intermediate-mass stars. If intermediate-mass stars dominate in the production of carbon, then the trend in C/O seen in Figure 3 could be interpreted as an "age" effect: the most metal-poor objects would be the youngest, displaying an enrichment pattern dominated by massive stars only, while the more metal-rich galaxies show increasing contributions from longer lived intermediate-mass stars.

2. *Variable yields.*—Recent stellar evolution models including mass loss via winds predict much larger yields of C relative to O (Maeder 1992; Woosley et al. 1993). If stellar winds are primarily radiatively driven, and dependent on opacity, then the stellar mass-loss rates should depend on metallicity. Maeder (1992) presents an analysis of the expected yields from stellar evolution models which incorporate metallicity-dependent stellar mass loss. These models result in an increasing yield of carbon, and a decreasing yield of oxygen, with metallicity, and thus, C/O increasing with O/H. Carigi (1994) has recently calculated chemical evolution models for the Galaxy which take the Maeder yields for massive stars into account. Her models show a significantly steeper increase in C/O with O/H than the older models of Matteucci & François (1989), which used massive star yields from Woosley (1986). We plot the results for Carigi's models 1a and 2 against our data in Figure 7. The models appear to reproduce the trend in the data fairly well, although there is a small systematic offset between the models and the data; this could indicate that the stellar yields require some adjustment, or that the observed carbon abundances are affected by grain depletion. Prantzos, Vangioni-Flam, & Chauveau (1994) have computed similar models for the solar neighborhood also, and find similar results.

One should use caution in using such models to interpret the observations at this time. Carbon yields are still relatively uncertain. The yields from massive stars are subject to uncertainties in convective mixing, nuclear reaction rates, and stellar mass-loss rates. Theoretical models suggest metallicity-dependent mass loss is important; observationally the situation is less certain. Direct measurements of stellar mass-loss rates have not been precise enough to demonstrate a correlation with Z, although indirect evidence from the frequency of Wolf-Rayet stars versus metallicity is more compelling (Leitherer 1993). Carbon yields for intermediate-mass stars, most commonly taken from Renzini & Voli (1981), have not been recomputed with the more recent estimates of the $^{12}C(\alpha, \gamma)^{16}O$ reaction rate, and so they are uncertain as well.

3. *Variable IMF.*—A variable stellar IMF has been invoked to explain some properties of giant H II regions and starburst galaxies (e.g., Melnick, Terlevich, & Eggleton 1985). If the IMF is weighted toward more massive stars at low metallicities, then an increasing C/O ratio with metallicity can be explained as a change in the relative contributions of massive and intermediate-mass stars. Observations of luminous stars in the Local Group show no convincing evidence for such a systematic variation in either the slope of the IMF or in the upper mass limit for stars (Garmany 1989; Parker & Garmany 1993). Moreover, varying the IMF affects the abundance ratios of a number of elements, as illustrated by models for sulfur presented in Garnett (1989). As a result, variable IMFs are not attractive for explaining variations in the composition of galaxies.

A comparison of Figures 3 and 4 proves interesting. Note in Figure 4 the abrupt drop in C/N between the solar neighborhood objects and the more metal-rich dwarf galaxies (NGC 2363 and LMC), attributable to much larger nitrogen abundances in the Galactic nebulae. In contrast, the C/O ratio maintains a smooth upward trend including the Galactic objects. Taken together, the features in Figures 3 and 4 suggest that the nucleosynthesis of C may be largely decoupled from that of N. One possibility is that C and O production is dominated by massive stars, while N comes mainly from intermediate-mass stars. Another possibility is that N and C both produced mainly in intermediate-mass stars, but in different mass ranges. The fluctuations in N/O could result from local pollution by Wolf-Rayet stars rather than delayed ejection of N from IMS (Pagel, Terlevich, & Melnick 1986; Pagel et al. 1992). At present it is not possible to design a unique model to account for the observed trends. The true picture will

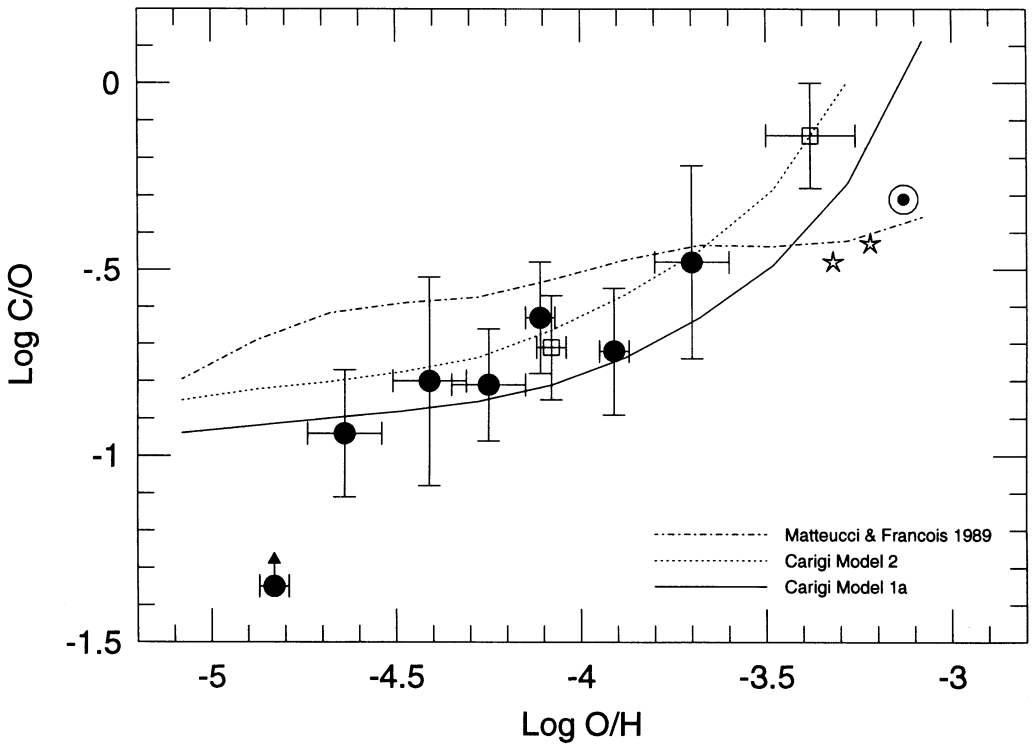

FIG. 7.—Comparison of C/O abundances in irregular galaxies with chemical evolution models from Carigi (1994) and Matteucci & François (1989); two of Carigi's models are represented by the solid and dotted lines; model 1a represents evolution for a Salpeter IMF, while model 2 is for a Scalo IMF. Both models use massive star yields from Maeder (1992). The Matteucci & François model is shown by the dot-dash line; this model uses massive star yields from Woosley (1986). Note that the chemical evolution models were designed to simulate the evolution of the solar neighborhood.

have repercussions for the use of $\Delta Y/\Delta$(element) correlations to determine the primordial He fraction (Steigman et al. 1989).

5. SUMMARY

We have presented UV spectroscopy of H II regions in low-luminosity dwarf galaxies and the Magellanic Clouds obtained with the Faint Object Spectrograph on the *Hubble Space Telescope*. We have measured O III] 1666 Å and C III] 1909 Å simultaneously, enabling us to determine C^{+2}/O^{+2} with greatly reduced uncertainties from errors in electron temperature and reddening. These FOS spectra represent a significant improvement over *IUE* in terms of sensitivity and reliability of abundance measurements. The results indicate that further FOS spectroscopy of H II regions will greatly improve our understanding of H II regions and the composition of the interstellar medium.

The results from our *HST* observations show a monotonic increase in log (C/O) from ~ -0.9 at log (O/H) ≈ -4.6 to ~ -0.5 at log (O/H) ≈ -3.7. This trend is different from that seen in the Galactic stars, where C/O is roughly constant at log (C/O) $= -0.9$ over the same range in O/H. One possible interpretation of this trend is that the most metal-poor galaxies are the youngest and dominated by the products of early enrichment by massive stars, while more metal-rich galaxies show increasing, delayed contributions of carbon from intermediate-mass stars. However, recent evolution models for massive stars including mass loss from stellar winds suggest that the yield of carbon from massive stars may increase with metallicity relative to the yield of oxygen, complicating the interpretation of the abundance trends.

The observed C/O ratios in our three most metal-poor galaxies are consistent with the estimate of Weaver & Woosley (1993) for the $^{12}C(\alpha, \gamma)^{16}O$ cross section. This result is subject to uncertainty from the poorly known contribution of carbon from intermediate-mass stars in these galaxies. Improved nucleosynthesis calculations for intermediate-mass stars are needed to enhance the interpretation of the observed trend in C/O.

The abrupt drop in C/N between 30 Dor and the solar neighborhood (Fig. 4) is intriguing. The result suggests that most of the nitrogen production in our Galaxy is delayed with respect to both carbon and oxygen, in contrast with previous results indicating that C and N varied in lockstep (Pagel 1985). It may be that Figure 4 indicates that spirals and irregulars experience different chemical evolution histories, and that one cannot safely combine abundance data from both irregulars and spirals to study the abundance evolution of every element. Certainly, more FOS observations of carbon are needed to confirm the trend in Figure 4, particularly measurements in H II regions in spiral galaxies.

Another question not addressed here is that of the intrinsic dispersion in C/O. It has been suggested often (e.g., Clayton & Pantelaki 1993; Pilyugin 1992, 1993) that dwarf galaxies experience intermittent starbursts, and that as a result the delayed ejection of fresh N and C from intermediate-mass stars should lead to relatively large fluctuations in N/O and C/O at fixed O/H. The data in Figure 3 suggest only a small intrinsic dispersion in C/O, but the sample is small, the uncertainties are still relatively large, and the target selection may have been fortuitous. FOS measurements of C/O for a larger sample of

dwarf galaxies would permit us to address the dispersion in C/O with greater confidence.

This study has benefitted from conversations with R. Bohlin, J. Cardelli, W. D. Arnett, K. Nomoto, and J. Mathis. We thank Leticia Carigi for providing us with machine-readable tables of her chemical evolution model results, and Bernard Pagel for helpful comments on the manuscript. We also thank Mike Potter of STScI for instructing us in the use of GASP at STScI. Support for this work was provided by NASA through grant GO-3840.01-91A from the Space Telescope Science Institute, which is operated by the Association of Universities for Research in Astronomy, Inc., for NASA under NAS 5-26555. Support for D. R. G. is provided by NASA and STScI through the Hubble Fellowship award HF-1030.01-92A. E. D. S. acknowledges support from NASA-LTSARP grant NAGW-3189. E. D. S., E. T., and R. J. T. acknowledge support from a NATO grant for Collaborative Research, No. CRG 910269.

REFERENCES

Aggarwal, K. 1983, MNRAS, 202, 15P
Aller, L. H. 1984, Physics of Thermal Gaseous Nebula (Dordrecht: Reidel)
Anders, E., & Grevesse, N. 1989, Geochim. Cosmochim. Acta, 53, 197
Arnett, W. D. 1971, ApJ, 170, L43
Baluja, K. L., Burke, P. G., & Kingston, A. E. 1981, J. Phys. B, 14, 119
Berrington, K. A. 1985, J. Phys. B, 18, L395
Berrington, K. A., Burke, P. G., Dufton, P. L., & Kingston, A. E. 1977, J. Phys. B, 10, 1465
Blum, R. D., & Pradhan, A. K. 1992, ApJS, 80, 425
Buchmann, L., et al. 1993, Phys. Rev. Lett., 70, 726
Burke, P. G., Lennon, D. A., & Seaton, M. J. 1989, MNRAS, 236, 353
Calzetti, D., Kinney, A., & Storchi-Bergmann, T. 1994, ApJ, 429, 582
Campbell, A., Terlevich, R., & Melnick, J. 1986, MNRAS, 223, 811
Cardelli, J. A., Mathis, J. S., Ebbets, D. C., & Savage, B. D. 1993, ApJ, 402, L17
Carigi, L. 1994, ApJ, 424, 181
Caughlan, G. A., & Fowler, W. A. 1988, Atom. Data Nucl. Data, 40, 238 (CF88)
Charbonnel, C., Meynet, G., Maeder, A., Schaller, G., & Schaerer, D. 1993, A&AS, 101, 415
Clayton, D. D., & Pantelaki, I. 1993, Phys. Rep., 227, 93
Clegg, R. E. S., Lambert, D. L., & Tomkin, J. 1981, ApJ, 250, 262 (CLT81)
Cunha, K., & Lambert, D. L. 1992, ApJ, 399, 586
———. 1994, ApJ, 426, 170 (CL94)
Dufour, R. J., Garnett, D. R., & Shields, G. A. 1988, ApJ, 332, 752 (DGS88)
Dufour, R. J., & Hester, J. J. 1989, ApJ, 350, 149
Dufour, R. J., Schiffer, F. H., & Shields, G. A. 1984, in Future of Ultraviolet Astronomy Based on Six Years of *IUE* Research, ed. J. Mead, R. Chapman, & Y. Kondo (Washington, DC: NASA) (CP-2349), 111 (DSS84)
Dufton, P. L., Berrington, K. A., Burke, P. G., & Kingston, A. E. 1978, A&A, 62, 111
Fitzpatrick, E. L. 1985, ApJ, 299, 219
Garmany, C. D. 1989, in Massive Stars in Starbursts, ed. C. Leitherer, N. R. Walborn, T. M. Heckman, & C. A. Norman (Cambridge: Cambridge Univ. Press), 115
Garnett, D. R. 1989, ApJ, 345, 282
———. 1990, ApJ, 363, 142
———. 1992, AJ, 103, 1330
Gies, D. R., & Lambert, D. L. 1992, ApJ, 387, 673 (GL92)
Gonzalez-Delgado, R. M., et al. 1994, ApJ, 437, 239
Grevesse, N., & Noels, A. 1993, in Origin and Evolution of the Elements, ed. N. Prantzos, E. Vangioni-Flam, & M. Casse (Cambridge: Cambridge Univ. Press), 15
Jenkins, E. B. 1987, in Interstellar Processes, ed. D. J. Hollenbach & H. A. Thronson (Dordrecht: Reidel), 533
Kilian, J. 1992, A&A, 262, 171 (K92)
Leitherer, C. 1993, in The Feedback of Chemical Evolution on the Stellar Content of Galaxies, ed. D. Alloin & G. Stasińska (Paris: Observatoire de Paris), 241
Lester, D. F., Dinerstein, H. D., Werner, M. W., Watson, D. M., Genzel, R. L., & Storey, J. W. V. 1987, ApJ, 320, 573
Maeder, A. 1990, A&AS, 84, 139
———. 1992, A&A, 264, 105
Mathis, J. S. 1990, ARA&A, 28, 37
Mathis, J. S., Chu, Y.-H., & Peterson, D. E. 1985, ApJ, 292, 195
Matteucci, F. 1986, MNRAS, 221, 911
Matteucci, F., & Tosi, M. 1985, MNRAS, 217, 391
Matteucci, F., & François, P. 1989, MNRAS, 239, 391
McGaugh, S. S. 1991, ApJ, 380, 140
Melnick, J., Terlevich, R. J., & Eggleton, P. P. 1985, MNRAS, 216, 255
Mendoza, C. 1983, IAU Symp. 103, Planetary Nebulae, ed. D. R. Flower (Dordrecht: Reidel), 103
Meyer, J.-P. 1985, ApJS, 57, 151
Mihalas, D. 1972, Non-LTE Model Atmospheres for B and O Stars (NCAR TN/STR-76)
Osterbrock, D. E. 1989, Astrophysics of Gaseous Nebulae (Mill Valley: University Science Books)
Pagel, B. E. J. 1985, in Production and Distribution of C, N, O Elements, ed. I. J. Danziger, F. Matteucci, & K. Kjar (Munich: ESO), 155
Pagel, B. E. J., Simonsen, E. A. Terlevich, R. J., & Edmunds, M. G. 1992, MNRAS, 255, 325
Pagel, B. E. J., Terlevich, R. J., & Melnick, J. 1986, PASP, 98, 1005
Panagia, N. 1973, AJ, 78, 929
Parker, J. W., & Garmany, C. D. 1993, AJ, 106, 1471
Peimbert, M., Peña, M., & Torres-Peimbert, S. 1986, A&A, 158, 266
Peimbert, M., Torres-Peimbert, S., & Dufour, R. J. 1993, ApJ, 418, 760
Pilyugin, L. S. 1992, A&A, 260, 58
———. 1993, A&A, 277, 42
Prantzos, N., Vangioni-Flam, E., & Chauveau, S. 1994, A&A, 285, 132
Prévot, M. L., Lequeux, J., Maurice, E., Prévot, L., & Rocca-Volmerange, E. 1984, A&A, 132, 389
Reimers, D., Vogel, S., Hagen, H.-J., Engels, D., Groote, D., Wamsteker, W., Clavel, J., & Rosa, M. J. 1992, Nature, 360, 561
Renzini, A., & Voli, M. 1981, A&A, 94, 175
Rolfs, C. E., & Rodney, W. S. 1988, Cauldrons in the Cosmos (Chicago: Univ. Chicago Press)
Rosa, M. A., & Benvenuti, P. 1994, A&A, 291, 1
Schaerer, D., Charbonnel, C., Meynet, G., Maeder, A., & Schaller, G. 1993b, A&AS, 102, 339
Schaerer, D., Meynet, G., Maeder, A., & Schaller, G. 1993a, A&AS, 98, 523
Schaller, G., Schaerer, D., Meynet, G., & Maeder, A. 1992, A&AS, 96, 269
Seaton, M. J. 1979, MNRAS, 187, 73P
Shields, G. A. 1990, ARA&A, 28, 525
Shields, G. A., Aller, L. H., Czyzak, S., & Keyes, C. D. 1981, ApJ, 248, 569
Shields, G. A., & Searle, L. 1978, ApJ, 222, 821
Skillman, E. D. 1991, PASP, 666, 919 (S91)
Skillman, E. D., & Kennicutt, R. C., Jr. 1993, ApJ, 411, 655
Sneden, C., Lambert, D. L., & Whitaker, R. W. 1979, ApJ, 234, 964 (SLW79)
Sofia, U. J., Cardelli, J. A., & Savage, B. D. 1994, ApJ, 430, 650
Stasińska, G. 1990, A&AS, 83, 501
Steigman, G., Gallagher, J. S., & Schramm, D. N. 1989, Comm. Astrophys., 15, 97
Terlevich, R. J., & Melnick, J. 1985, MNRAS, 213, 841
Tielens, A. G. G. M., & Allamandola, L. J. 1987, in Interstellar Processes, ed. D. J. Hollenbach & H. A. Thronson (Dordrecht: Reidel), 397
Tinsley, B. M. 1979, ApJ, 229, 1046
Tomkin, J., Lemke, M., Lambert, D. L., & Sneden, C. 1992, AJ, 104, 1568 (TLLS92)
Torres-Peimbert, S., Peimbert, M., & Daltabuit, E. 1980, ApJ, 238, 133
VandenBerg, D. A. 1985, in Production and Distribution of the CNO Elements, ed. I. J. Danziger, F. Matteucci, & K. Kjar (Munich: ESO), 73
Walter, D. K., Dufour, R. J., & Hester, J. J. 1992, ApJ, 397, 196
Weaver, T. A., & Woosley, S. E. 1993, Phys. Rep. 227, 65 (WW93)
Wheeler, J. C., Sneden, C., & Truran, J. W. 1989, ARA&A, 27, 279
Woosley, S. E. 1986, in Nucleosynthesis and Chemical Evolution, ed. B. Hauck, A. Maeder, & G. Meynet (Geneva: Geneva Observatory), 1
Woosley, S. E., Langer, N., & Weaver, T. A. 1993, ApJ, 411, 823
Zhao, Z., France, R. H., III, Lai, K. S., Rugari, S. L., & Gai, M. 1993, Phys. Rev. Lett., 70, 2066